Investigation of Structural, Thermal and Magnetic properties of Strontium substituted Barium Hexaferrite Synthesized via co-precipitation Method

S.Vadivelan*, N.VictorJaya

Department of physics, Anna University, Chennai-25, India

Abstract: In this paper, the strontium doped barium hexaferrite ($BaSr_xFe_{12-x}O_{19}$) is synthesized by co-precipitated technique and involved the sintering process (1000°C up to 5hrs). After that the properties of these prepared samples are analyzed using various characterizations. The barium hexaferrite is mostly used in recording devices as well as permanent magnetic materials, because it exhibits perfect magnetic properties. The pure and strontium doped (X=1%, 3%, 5% and 7%) barium hexaferrite were obtained from the technique. The x-rd peaks were indexed as a primitive hexagonal cell with the refined lattice parameter values of a=b=5.865 Å, and c=23.099 Å. From the lattice parameter values the structure of this compound is hexagonal. TGA/DTA is the studies to analysis the degradation mechanisms, reaction kinetics, determination of organic content and determination of inorganic (e.g. ash) content in a sample around 850°C and transformation of residuals at the around temperature 585°C. From the FT-IR, the functional groups and vibration modes are identified. SEM image is confirmed the size of the particles of the sample. From VSM characterization, the magnetic saturation (Ms) Value is increasing from 10.9-33.9emu/g with increasing doped percentage of strontium and magnetic remanenc (Mr) increased from 3.98-24.95 emu/g with increasing doped percentage of strontium. Hc value of pure and doped barium hexaferrite also calculated and summarized in the table.

Keywords: co-precipitation, barium hexaferrite, saturation magnetization, magnetic remanence.

1. Introduction

Barium ferrite (BaFe) is a highly magnetic material and high packing density. Recently the ferrite materials are used in magnetic card strips, speakers, and magnetic tapes. Particularly long term data storage device are found successfully. These materials are resistant to temperature, corrosion, and oxidization properties. The material has proven to be resistant to a number of different environmental stresses, including humidity and corrosion. Because Ferrites are already oxidized it cannot be oxidized any further. This is one reason Ferrites are so resistant to corrosion [1-3]. Barium ferrite also proved to be resistant to thermal demagnetization, another issue common with long term storage. When the temperature increases the coercivity value greatly increased. This behavior makes it more resistant to thermal demagnetization. Due to this characteristic of Barium Ferrite makes it a popular choice in motor and generator designs and also in loudspeaker applications. Ferrite magnets are extremely good insulators and don't allow any electrical current to flow through them and they are brittle which shows their ceramic characteristics [4-5].

Ferrite magnets also have good machining properties, which allows for the material to be cut in many shapes and sizes. Barium ferrites are robust ceramics that are generally stable to moisture and corrosion resistant. Barium ferrite is a very applicable material used in many industry fields. The material is seen around the world in applications such as recording items such as tapes and other media devices, permanent magnets, and also magnetic stripe cards [6-8]. Due to the stability of the material, it is able to be greatly reduced in size, making the packing density much greater. The barium ferrite which has recently taken the oxide's place produces much higher coercivity levels which make the material magnetically hard, therefore making the ferrite better for recording materials. As talked about earlier, these magnetic stripe cards and their readers are implanted with a unique pattern of barium ferrite [9-10].

In generally Barium ferrite is a common material for speaker magnets. The materials can be formed into almost any shape and size using a process called sintering whereby powdered barium ferrite is pressed into a mold, and then heated until it fuses together. The barium ferrite turns into a solid block while still retaining its magnetic properties. The magnets have an excellent resistance to demagnetization, allowing them to still be useful in speaker units over a long period of time. The packing density of barium ferrite is increased with increased the surface area of the materials [11-12]. Due to this property the data can be recorded more in the materials. The main aim of this work is increased the storage capacity of the barium ferrite materials. Storage capacity of the barium ferrite materials is to be increased due to magnetic material is doped with various percentages.

Strontium is a more magnetic and stability material so that it can be used a doped material with various percentages. The divalent transition metals such as $Co^{2+/3+}$, $Ni^{2+/3+}$ and $Sr^{2+/3+}$ for $Fe^{2+/3+}$. These are frequently used due to their similarity in ionic radius and electronic configurations [13-14]. The magnetic and dielectric properties depend on the preparation technique as well as structure of this compound. However, the co-precipitation technique is a better technique to examine the properties of the compound.

2. Experimental

2.1 Material and methods

The strontium doped barium hexaferrite are prepared by co-precipitation method with various doping percentage. The raw materials of the barium nitrite, iron nitrate, strontium nitrate, citric acid and NH_3 were taken in the required ratio with the distilled water. The ammonium hydroxide is used to regulate the synthesized process. The mixtures of the raw materials were stirrer at 60°C up to 2hrs. The prepared solution is washed 3 or 4 times with distilled water and ethanols separately because of the dust particles are removed. Finally strontium doped barium hexaferrite is prepared in the form of powder particles. The prepared powder samples are involved the sintering process at the temperature 1000°C up to 5 hrs. After sintering process, the sintered powder samples are concerned the grinding process up to nanoparticle size.

3. Result and discussion

3.1. X-ray diffraction (XRD) analysis

The structure and composition analyses were carried out by powder X-ray diffraction. X-rd patterns for the samples is 0%, 1%, 3% , 5% , and 7% of strontium doped barium hexaferrite were recorded in the region of 2θ=10-80° with a step scan of 0.02°/min on a PANalytical X"pert PRO X-ray diffractometry using CuKα radiation. JCPDS 78-0133 diffraction files were used to match the evolving phases [15-16]. The strong diffraction peaks of pure and strontium doped barium hexaferrite samples exhibit standard peaks at 2θ values corresponding to (110), (107) and (114) planes respectively. Cell parameters were calculated and also refined using linear regression procedures applied to the measured peak positions of all major reflections up 90°
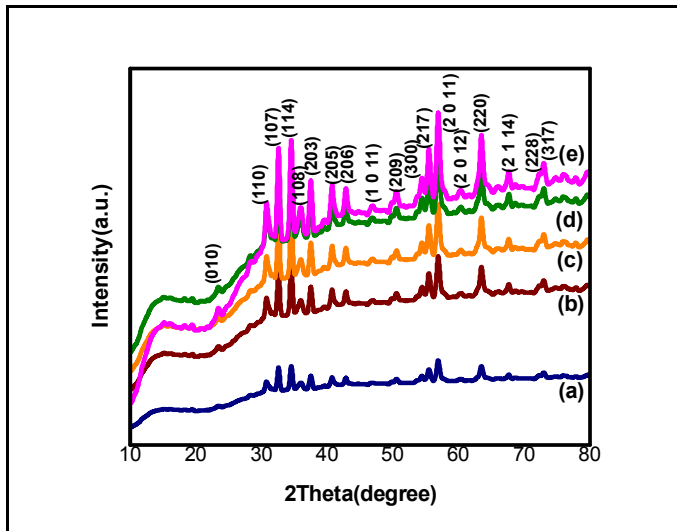
Fig. 2. XRD pattern of pure and strontium doped barium hexaferrite powder samples.

The crystallite size was determined from the diffraction profile of the strongest peak by using Scherrer formula t= $(k\lambda/\beta\cos\theta)$ [17-19]. Where k=Scherrer constant (k=0.9), t= average size of the crystallite, λ=wavelength of radiation (λ=1.54056Å), β=full width half maximum of the diffraction peak at θ and θ=diffraction angle corresponds to the peak position measured in radian as shown in fig.2. The average crystalline size 't' and lattice constants are calculated and summarized in table no. 1. From the above tabulation we concluded that the crystalline size of the samples is decreased with increased in doped percentage of strontium.

	Average crystalline size 't'(nm)	Lattice Constant (a) (Å)	Lattice Constant (c) (Å)
Pure	36.5	5.864	23.099
Sr 1%	34.6	5.862	23.094
Sr 3%	33.2	5.868	23.101
Sr 5%	32.8	5.864	23.099
Sr 7%	31.4	5.862	23.101

3.2. Thermogravimetric (TGA) / Differential thermal (DTA) analysis

TGA/DTA is commonly used to determine the characteristics of materials that exhibit either mass loss or gain due to decomposition and oxidation. From this studies, the degradation mechanisms, reaction kinetics, determination of organic content and determination of inorganic (e.g. ash) content are analyzed in a samples. The fig.2 shows that, the pure and doped barium hexaferrite [20-22].
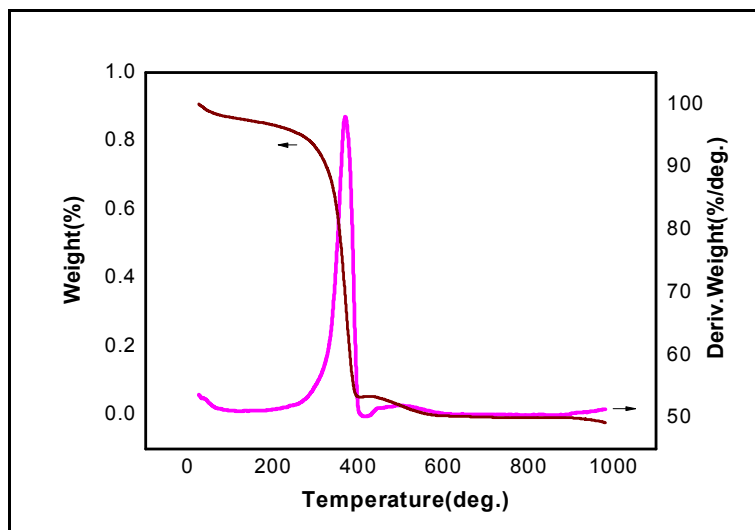
Fig.2 TGA/DTA curve for pure barium hexaferrite powder sample.

The weight loss is incremental and an overall loss of about 7% is indicated. There is an appearance of an endothermic in the DTA curve at 810°C. The peak is attributed to the decarboxilation of BaCO3, reported to take place at 1050°C for pure carbonate and around 800°C for the mixture of carbonate and iron oxide [23-24]. The completion of the formation of the hexaferrite is indicated at around 1045°C and 1010°C for the barium ferrite. The exothermic DTA curve indicates that, residual of Co_3O_4 to Co_2O_3 transformations at the temperature is 580°C.

3.3 Fourier transforms infrared spectroscopy (FT-IR) analysis

From the FT-IR spectrum high and low frequency absorption bands corresponding to stretching vibrations are analyzed. The absorption peaks purely depend on the crystalline nature, morphology and chemical composition of the materials in order to determine the chemical bonding nature of pure and Sr doped $BaFe_{12}O_{19}$ compounds [25-28]. The fig. 3 shows that the FT-IR spectrum of pure and strontium doped barium hexaferrite and its exhibited the functional groups and intense absorption band appeared between the frequencies regions of 400–1070 cm^{-1}, characterizes the deformation modes of Sr–O and Fe–O. In addition, the absorption band below 500 cm^{-1} is due to the deformation of Fe–O bonds in the deformation of Fe–O–Fe bridges [29].
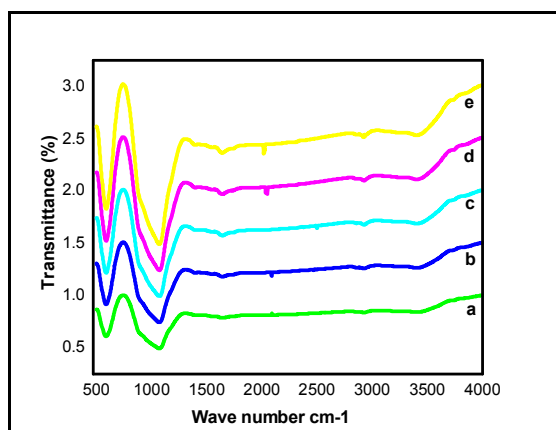

Fig.3 FT-IR spectrum of pure and strontium doped barium hexaferrite powder samples.

From the fig.3 a, b, c, d and e denotes the pure and strontium doped percentage 1%, 3%, 5%, 7% respectively. The bands at 1630, 2010 and 2600 cm^{-1} are caused by flexural vibrations of -OH groups. It is identified that the surface of the samples exist active -OH groups. The vibration of Fe-O is in the frequency band range at low frequency wave number is 472-524 cm^{-1} .For sintered sample, the IR band at 3455 and 1637

S.Vadivelan _et al_ /Int.J. ChemTech Res. 2015,8(12),pp 404-410.

408

cm^{-1} can be assigned to the vibration of -OH groups and the samples have some relocation [30]. Meanwhile, the relative strength of peak has also changed. This may be caused by -OH removes through sintering.

3.4. Scanning electron microscopy (SEM) analysis

The morphology of the pure and doped barium hexaferrite was examined by scanning electron microscope (JEOL JJM 6060). The scanning electron microscope was used to determine the particle size as well as to observe the microstructure features of the particles [31-32].The size and shape of strontium doped barium hexaferrite is analyzed by SEM characterization as shown in fig. 4.
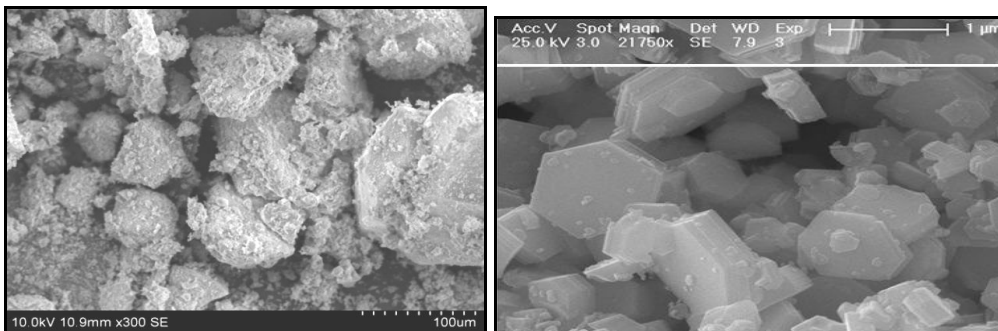

Fig.4 SEM image of strontium doped (1%) barium hexaferrite powder particles.

3.5. Vibrating sample magnetometer (VSM) analysis

A vibrating sample magnetometer (VSM, Lakeshore 736 and 7400 Series) for magnetic measurement was used to analyze the magnetic properties of the samples [33-35]. The pure and doped barium hexaferrite samples (0%, 1%, 3%, 5% and 7%) are involved the magnetic measurement. The resulting hysteresis loops obtained from the relation between magnetization (M), and the applied field (H), at temperatures of 27°C by means of a helium cooled 12T super-conducting magnet. Thus, the parameters are extracted from the hysteresis loop like saturation magnetization (Ms), remanence (Mr), coercivity (Hc) and squareness ratio (SQR) which in turn is related to the slope at Hc of the Sr doped barium hexaferrite samples are determined by using VSM results. The hysteresis loops as shown in fig. 5 for the pure and strontium doped barium hexaferrite. From the VSM studies to analyze the magnetic saturation (Ms), magnetic remanence (Mr) and coercivity (Hc) with high field (H) is applied [36]. To find the remanence magnitude can be calculated /extracted from the hysteresis curve at the intersections of the curve with the axis of vertical magnetization.
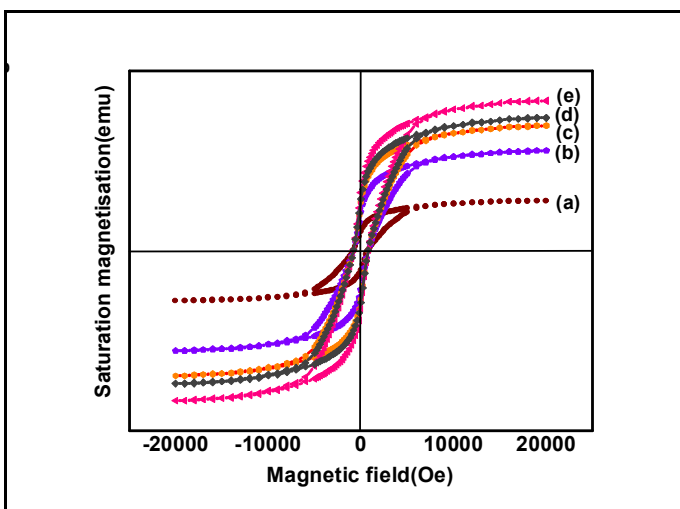

Fig. 5 Hysteresis curve for pure and strontium doped barium hexaferrite powder samples.

The remnant magnetization (Mr), magnetic saturation (Ms), coercivity (Hc) and squareness ratio (SQR) at 300K for pure and strontium doped barium hexaferrite is summarized in table no.2. (37-38). Squareness (SQR) values of these samples are calculated by this ratio (Mr/ Ms).

Table. No 2

Sample	Saturation (Ms) (emu/g)	Remnant(Mr) (emu/g)	Squareness (Mr/Ms)	Coercivity(Hc) (Oe)
Pure	10.9	3.98	0.365	789.153
Sr 1%	23.4	8.59	0.367	791.365
Sr 3%	28.8	10.95	0.380	793.568
Sr 5%	30.5	11.85	0.388	795.532
Sr 7%	33.9	24.95	0.735	799.658

In generally, large SQR values are preferred in many magnetic storage applications such as magnetic recording media of high density. From the analysis the temperature increased simultaneously SQR value also increased gradually. From the SQR and Hc calculation we conclude that the strontium doped percentage is increased greatly with increased the SQR values. The Based on density of the samples, SQR and coercivity value is varied. The more percentage of strontium doped barium hexaferrite materials can exhibit a higher magnetization and magnetic storage capacity. This is due to fact that the samples were not sintered in the presence of magnetic field [39-41].

4. Conclusions

From the XRD studies, the various ratio of strontium doped barium hexaferrite ($BaSr_xFe_{12-x}O_{19}$) is confirmed the structure of these samples is hexagonal. TGA/DTA result explains completion of the formation of barium hexaferrite is indicated at the temperature around 845°C and 925°C for the barium hexaferrite. The functional groups, bonds and vibration mode of the samples are investigated by FT-IR characterization and the resultant spectra are presented with clearly above. SEM analysis clearly presented the structure of pure and strontium doped barium hexaferrite is hexagonal. The magnetic properties of pure and various percentages of $Sr^{2+/3+}$ doped barium hexaferrite have been showed. From the tabulation we concluded that the percentage of strontium is increased as well as greatly increased magnetic storage capacity. The storage capacity is depends up on only magnetic properties of the samples. From the table no 2, we concluded that the remnant magnetization (Mr), magnetic saturation (Ms), coercivity (Hc) and squareness ratio (SQR) are depends only doped percentage of strontium. The magnetic properties of the sample are affected greatly through the preparation and sintering process. Compare to other technique the co-precipitated technique is very excellent technique to prepare the magnetic storage materials. This type of ferrite materials are widely used in subwoofer medium for magnetic recording, storage devices, magneto-optic media, telecommunication, electronic industry etc.

References

1. A. Mali, A. Ataie, Ceram Int., 30 (2004) 1979–1983.
2. A. Ghasemi, A. Saatchi, M. Salehi, A. Hossienpour, A. Morisako, X. Liu, Phys Status Solidi A, 10 (2006) 2513–2521.
3. Z. Haijun, L. Zhichao, M. Chengliang, Y. Xi, Z. Liangying, W. Mingzhong, Mater Chem Phys., 80 (2003) 129–134.
4. G. Mendoza-Suarez, L. P. Rivas- Vazquez, J. C. Corral-Huacuz, A. F. Fuantes, J. I. Escalante-Garcia, Physica B, 339 (2003) 110–118.
5. H. Hua, S. Z. Li, Z. D. Han, D. H. Wang, M. Lu, W. Zhong, B. X. Gu, Y. W. Du, Mat. Sci. Eng A-Struct, 448 (2007) 326–329.
6. G. Mendoza-Suarez, L. P. Rivas- Vazquez, A. F. Fuantes, J. I. Escalante-Garcia, O. E. Ayala-Valenzuela, E. Valdez, Mater. Lett., 57(2002) 868–872.
7. J. Zhou, H. Ma, M. Zhong, G. Xu, Z. Yue, Z. He, J Magn Magn Mater., 305 (2006) 467–469.
8. R. D. Waldrons, "The Infrared Spectra of Ferrites," *Phys-ics Review*, 99 (1955) 1727-1735.

9.   F. L. Wei, H. C. Fang, C. K. Ong, et al., J. Appl. Phys., 87 (2000) 8636–8639.
10. M. A. Mousa and M. A. Ahmed, "Electrical Conduction in *γ*-Irradiated and Unirradiated Zinc-Iron Ferrites," *Chemistry and Material Science*, 23 (1988) 3083-3087.
11. O. S. Josyulu and Sobhanadri, "The Far-Infrared Spectra of Some Mixed Cobalt Zinc and Magnesium Zinc Fer-rites," *Physica Status Solidi* (*a*), 65 (1981) 479-483.
12. Y. Liu, M. G. B. Drew, J. Wang, M. Zhang, Y. Liu, J. Magn. Magn. Mater. 322 (2010) 366-367.
13. Y. Liu, M. G. B. Drew, Y. Liu, J. Wang, M. Zhang, J. Magn. Magn. Mater. 322 (2010) 3342-3343.
14. Z. W. Li, C. K. Ong, Z. Yang, F. W. Wei, X. Z. Zhou, J. H. Zhao, A.H. Morrish, Phys. Rev. B, 62 (2000) 6530–6537.
15. O. Kubo, T. Ido, and H. Yakoyama, IEEE Trans. Magn. 18 (1982) 1122-1123.
16. Z. Yang, J. H. Zhao, H. X. Zeng, G. Yan, Int. J. Soc. Mater. Eng.Resour., 3 (1995) 203-204
17. Z. Haijun, L. Zhichao, M. Chengliang, Y. Xi, Z. Liangying, W. Mingzhong,   Mater. Sci. Eng. B, 96 (2002) 289–295.
18. L. Dong, Z. Han, Y. Zhang, Z. Wu, Z. Zhang, Rare Metals, 25 (2006) 605–608.
19. A. Ghasemi, X. Liu, A. Morisako, J Magn Magn Mater., 316 (2007) 105–108.
20. O. Carp, R. Barjega, E. Segal, M. Brezeanu, Thermochim Acta, 318 (1998) 57–62.
21. A. Hakola, O. Heczko, A. Jaakkola, T. Kajava, K. Ullakko, ApplPhys A, 79 (2004) 1505–1508.
22. S. T. Park, W. Kang, H. T. Kim, S. J. Yun, B Korean Chem Soc., 293 (2008) 685–688.
23. J. Ding, W. F. Miao, P. G. McCormick, R. Street, J Alloy Compd.,281 (1998) 32–36.
24. W. Zhong, W. Ding, N. Zhang, J. Hong, Q. Yan, Y. Du, J Magn Magn Mater., 168 (1997) 196–202.
25. N.Kishan Reddy et al., "Magnetic properties of W-type ferrites", Materials chemistry and Physics, 76 (2002) 75-77.
26. D. Miha, K. Matjaž, H. Darko, L. Darja, J. Am. Ceram.Soc 90 (2007) 2057-2061.
27. X. H. Huang, Z. H. Chen, Scripta Mater., 54 (2006) 169–173.
28. H. Sözeri, Z. Durmus, A. Baykal, E. Uysal, Mater. Sci.Eng. B 177 (2012) 949-955.
29. A. Ghasemi, A. Saatchi, M. Salehi, A. Hossienpour, A. Morisako, X.Liu,   Phys Status Solidi A, 10 (2006) 2513–2521.
30. A. Collomb, B. Lambert-Andron, J.X. Boucherle, D. Samaras, Phys.Stat. sol. (A) 96 (1986) 385.
31. S.K. Mandal, K. Singh, D. Bahadur, J. Mater. Sci. 29 (1994) 3738
32. J. Ding, W.F. Miao, P.G. McCormick, R. Street, Highcoercivity ferrite magnets prepared by mechanical alloying, Journal of Alloys and Compounds 281 (1998) 32-36.
33. P.E. Garcia-Casillas, A.M. Beesley, D. Bueno, C.A. Martinez, Remanence properties of barium hexaferrite, Journal of Alloys and Compounds 369 (2004) 185-189.
34. S. Foner, Versatile and sensitive vibrating-sample magnetometer, Revision Science Instruments 30 (1959) 548-557.
35. R. Nowosielski, R. Babilas, G. Dercz, L. Pajak,Microstructure of composite material with powders of barium ferrite, Journal of Achievements in Materials and Manufacturing Engineering 17 (2006) 117-120.
36. S. Ram, H. Krishnan, K.N. Rai, K.A. Narayan, Japanese J. Appl. Phys. 28 (4) (1989) 604.
37. R.D. Shannon, Acta Crystallogr. A 32 (1976) 751.
38. C. Duval, Inorganic Thermogravimetric Analysis, Elsevier, London,(1963) 533.
39. Y.S. Homg, C.M. Ho, H. Y Hsu, C.T. Liu, J. Magn. Magn. Mater.279 (2004) 401.
40. G. Benito, M.P. Morales, J. Requena, V. Raposo, M. Vazquez, J.S.Moya, J. Magn. Magn. Mater. 234 (2001) 65–72.
41. G.C. Bye, C.R. Howard, J. Appl. Chem. Biotechnol. 21 (1971) 319.

*****